

First-Passage Percolation, Semi-Directed Bernoulli Percolation, and Failure in Brittle Materials

L. Berlyand,¹ M. D. Rintoul,² and S. Torquato²

Received May 28, 1997; final November 26, 1997

We present a two-dimensional, quasistatic model of fracture in disordered brittle materials that contains elements of first-passage percolation, i.e., we use a minimum-energy-consumption criterion for the fracture path. The first-passage model is employed in conjunction with a "semi-directed" Bernoulli percolation model, for which we calculate critical properties such as the correlation length exponent ν^{sdir} and the percolation threshold p_c^{sdir} . Among other results, our numerics suggest that ν^{sdir} is exactly 3/2, which lies between the corresponding known values in the literature for usual and directed Bernoulli percolation. We also find that the well-known scaling relation between the "wandering" and energy fluctuation exponents breaks down in the vicinity of the threshold for semi-directed percolation. For a restricted class of materials, we study the dependence of the fracture energy (toughness) on the width of the distribution of the specific fracture energy and find that it is quadratic in the width for small widths for two different random fields, suggesting that this dependence may be universal.

KEY WORDS: First-passage percolation; semi-directed percolation; fracture; brittle materials.

1. INTRODUCTION

An understanding of how materials fail and the prevention of such failures is one of the most important problems in modern materials research. Theoretical studies on this subject go back to the classical works of Griffith,⁽¹⁾ Inglis,⁽²⁾ and Irwin.⁽³⁾ Phenomenological models of this process abound.^(4, 5) Recent progress on this subject has been achieved by using the powerful theoretical and computational methods of statistical mechanics.^(6, 7) In this

¹ Department of Mathematics, Pennsylvania State University, University Park, Pennsylvania 16802.

² Princeton Materials Institute and Department of Civil Engineering and Operations Research, Princeton University, Princeton, New Jersey 08540.

paper we attempt to study some features of brittle fracture in two dimensions using well-known ideas and methods of percolation theory in combination with numerical simulations. In the course of this study, a number of questions arose that are of interest and relevance to percolation theory itself and which we answered using numerical simulations.

Percolation theory serves as a guide for the understanding of a wide variety of processes in nature such as transport processes in random media, the spreading of epidemics and fires, statistical tomography, and many others. As is well known, the simplest “Bernoulli” percolation model can be formulated as follows. Consider a periodic hypercubic lattice in d -dimensional space whose bonds (sites) are occupied or vacant with probabilities p or $1 - p$, independently of one another. For a given realization of occupied and vacant bonds (sites), two vertices of the lattice are said to be connected if they can be joined by a path consisting of occupied bonds only. Depending on the definition of connectedness, one can define other percolation models. In this paper we shall deal with short-range percolation models on a two-dimensional regular or random lattice. We recall that the *percolation threshold* is a positive number $p_c < 1$ (its value depends on d and the notion of connectedness) such that for $p < p_c$, there are no infinite connected sets of edges, while for $p > p_c$ a unique connected set (also called the infinite cluster) exists (see refs. 8–10 and references therein.)

The methods and ideas of percolation theory have been used in the modeling of fracture by many authors. Various lattice percolation methods have been applied to fracture models in which the medium is viewed as a set of bonds (springs) with randomly distributed breaking constants σ_c .^(7, 11) Under an applied load, the weakest bond breaks first, and then the stresses are redistributed among all remaining bonds. This procedure is repeated until all appropriate bonds are broken. One of the main objectives in such studies⁽⁷⁾ is the distinction between so-called global-load sharing models, where the load previously carried by a failed bond is shared equally by all remaining bonds, and so-called local sharing models in which the load is shared by the bonds in the immediate vicinity of the broken bond. Because of the redistribution mechanism, one must solve a large linear system of Kirchoff equations at each breaking step.

It is well known that fracture can be defined as the creation of new surfaces (cracks) within a body through application of external forces.⁽⁵⁾ The key quantity which determines the crack path under given external forces is the specific fracture energy $\gamma(x)$, i.e., the energy required for the creation of (two) new surfaces per unit area. In inhomogeneous materials such as composites, rocks, concrete and polycrystals, $\gamma(x)$ is a random field which could be characterized by some spatial probabilistic distribution. In two dimensions, Jeulin⁽¹²⁾ numerically found the trajectory of the path

between two prescribed points (source and destination) which minimizes total fracture energy $\gamma(x)$ along the path. This was determined solely from geodesic propagation, i.e., minimizing the distance with respect to the field $\gamma(x)$, which is equivalent to using the minimum energy consumption criterion only. Such a consideration is analogous to the well-known Fermat principle, in which the light trajectory in a heterogeneous medium is determined from the minimization of time criterion, i.e., the trajectory of light is a geodesic with respect to the metric determined by travel time. In Jeulin's studies the stored elastic energy field $G(x)$ (or energy release rate) was ignored; moreover, he did not characterize crack statistics using the exponents ζ and χ described below.

We consider modeling the failure of brittle materials when the quasi-static approximation holds. This enables us to use the well-developed results and ideas of the theory of *first-passage percolation*, originally invented by the mathematicians Hammersly and Welsh to model the spread of fluid through a porous media (see ref. 13 and references therein). Physically, this means that we restrict ourselves to the case when the applied load is not very high. (Indeed, it is known that at very high loads the dynamical effects dominate and the quasi static approximation based on energy consideration does not hold.⁽¹⁴⁾) We recall that for first-passage percolation processes^(8,15) each edge e of the lattice is assigned a random number $T(e)$ (time coordinate). For any path (set of connected edges with no self intersections) $\pi_{A,B}$ connecting vertices A and B , the time taken to travel from A to B is defined as $\sum_{e \in \pi} T(e)$. The first-passage time $T(A,B)$ is then defined as the minimum travel time over all paths joining A and B . One can also specify the orientation or direction of the paths between A and B .^(8,10) A *directed* path is one in which each edge is oriented in the direction of increasing coordinate value, i.e., "north-east" orientation. A *semi-directed* path is one in which each edge possesses north, east, or west orientation.

For our fracture model, we consider first-passage percolation in which energy plays the role of time and the crack paths are semi-directed since the paths cannot physically reverse themselves. Moreover, we employ the traditional Bernoulli percolation model but in a *semi-directed* manner to study the behavior of the cracks in the vicinity of the critical percolation threshold p_c^{dir} for a certain semi-directed model. To our knowledge, little is known about the critical properties (e.g., threshold p_c^{dir} and correlation length exponent ν^{dir}) for semi-directed Bernoulli percolation models. Most notably we have found that $\nu^{\text{dir}} = 3/2$, which our numerics suggest is an exact analytical value. This lies between the values of $\nu = 4/3$, for usual Bernoulli percolation, and $\nu^{\text{dir}} = 26/15$ (based on numerics), for directed percolation.

There are many physical phenomena that require finding the minimum (over all paths) of the sum of weights of paths connecting two end points, i.e., first-passage percolation. Such problems have been studied intensively in the statistical physics literature and include, among others, *directed polymers* in random media.⁽¹⁶⁾ For directed polymers and other interface problems,⁽¹⁷⁻¹⁹⁾ it has been demonstrated that the exponents ζ and χ are universal and are believed to take the values $2/3$ and $1/3$. The “wandering” exponent ζ characterizes how transverse fluctuations of the path scale with the distance L between the two endpoints, whereas the exponent χ describes how energy fluctuations scale with L . They also satisfy the scaling relation $\chi = 2\zeta - 1$. However, we emphasize that the values $2/3$ and $1/3$ and the scaling relation have been established away from criticality. Thus, an interesting question is whether the exponents remain universal in the vicinity of the threshold for the semi-directed percolation model. Here we show that by adding critical behavior to the semi-directed first-passage model, we can observe several new effects. In particular, we have found that the scaling relation $\chi = 2\zeta - 1$ breaks down in the vicinity of the percolation threshold.

The interpretation of semi-directed percolation and the associated exponents in the context of fracture of brittle solids suggested several interesting studies. In particular, we have determined numerically the dependence of the energy consumed by the fracture path on the width of the distribution of the random field $\gamma(x)$ (i.e., degree of inhomogeneity of the material). This dependence is found to be quadratic for small widths and two different distributions (uniform and Gaussian), suggesting that this dependence may be universal. In fact, it would be interesting to prove this result analytically using perturbation theory calculations. We remark here that if the material is such that the major crack dominates all others then the above result allows us to evaluate the fracture energy (and thus fracture toughness) as a function of the width distribution. Of course, for many materials, other processes off the crack path may consume a significant amount of energy, in which case this conclusion does not apply. We have also confirmed the fractal nature of the fracture path near criticality which was previously suggested by several authors. However, even though many numerical studies have confirmed fractality, it is still an open question from the mathematical point of view, i.e., a rigorous proof of the fact that the dimension of the path is strictly greater than unity has not been found yet (see note added in proof).

In Section II, we describe our two-dimensional fracture model in detail. In Section III, we determine critical parameters for semi-directed Bernoulli percolation. In Section IV, we quantitatively characterize the optimal fracture paths by calculating fluctuation exponents. Finally, in Section V, we make concluding remarks.

II. MATHEMATICAL MODEL

As a simple model example we consider a long plate of height L under a horizontal load (see Fig. 1a). Since information from an image of a material is most commonly stored in digitized form, it is convenient to use graph representations of the images.⁽¹²⁾ Therefore, we consider a part of the two-dimensional square lattice confined between two horizontal parallel lines a distance L apart (see Fig. 1b). The lattice spacing is assumed to be unity and to each edge (bond) e of the lattice a random number $\gamma(e)$ is assigned. This represents a discretization of the continuous random field $\gamma(x)$ of the local specific fracture energy. Similar models of random graphs on two-dimensional planes were studied by D. Jeulin.⁽¹²⁾ Note that the square symmetry of the lattice is chosen just to fix ideas. One can also study various types of periodic lattices (honeycomb and triangular) as well as random Poissonian mosaics. We emphasize that our lattice spacing is not representative of interatomic distances but rather represents the typical scale of inhomogeneities or variations of the random field $\gamma(x)$.

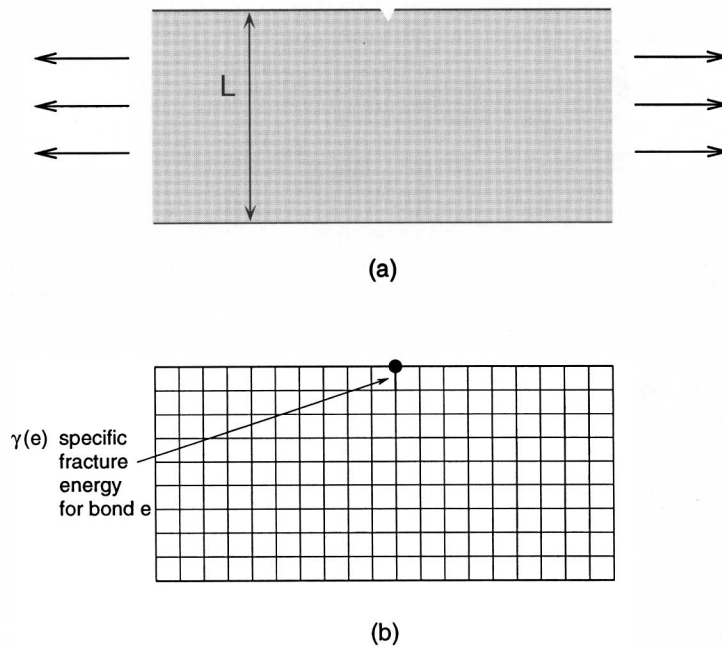


Fig. 1. Diagram of the system under study. (a) The system is under a horizontal load, and the crack it taken to propagate from the center of the top, to the bottom, breaking it into two pieces. (b) Lattice model of system.

We assume that our plate is a brittle random material. Let $G(x, y)$ be the energy release rate (stored elastic energy released in the loaded specimen). We consider the possible fracture paths $\Pi(L)$ which start at upper edge of plate and end at the lower edge of the plate, i.e. only those paths which actually break our specimen into two pieces. It follows from Griffith's criterion that a crack will grow if the energy release rate is greater than the energy to create a surface. For a lattice model, this means that for each bond e from the path $\Pi(L)$

$$2\gamma(e) < G(e), \quad e \in \Pi(L) \quad (1)$$

(see ref. 20 and references therein). Relation (1) assures that there is sufficient amount of potential energy released to compensate for the energy required for the formation of new surfaces (two surfaces). The energy release rate $G(x, y)$ depends on the loading conditions and the stress-strain relationship. Let us introduce the upper and lower bounds of the function $G(x, y)$ (or its discretization $G(e)$):

$$G_- \leq G(x, y) \leq G_+ \quad (2)$$

for all x and y .

We first consider the quasi-static case when $\gamma_{\max} = \max \gamma(e)$ among all bonds e satisfies the following condition:

$$2\gamma_{\max} < G_- \quad (3)$$

There are many paths which join the upper and lower edges of our plate. Our main objective is to find the fracture path (first crack which traverses the plate) and describe statistically its characteristics such as roughness, length, etc. We call this the *optimal fracture path* or OFP. In the case where Eq. (3) is valid, the OFP is entirely determined by the minimum energy consumption criterion, i.e. the OFP which starts at a fixed point $A = (x, L)$ on the upper edge $y = L$ and goes all the way down to the lower edge $y = 0$ minimizes the total fracture $\Gamma(L)$ energy along the path among all paths which join the point B and the lower edge. Here $\Gamma(L)$ is defined by

$$\Gamma(L) = \sum_{e \in \Pi(x, y)} \gamma(e) \quad (4)$$

The initial point A in a real physical problem can be prescribed by applying a point force at a particular point or by considering crack initiation from a small notch made on the upper edge, as is usually done in the experimental determination of the fracture toughness,⁽²¹⁾ (see Fig. 1a).

We emphasize that the endpoint of the path is not prescribed in our formulation; the path itself chooses it by minimizing $\Gamma(L)$. We note that in ref. 12 both ends (source and destination) of the minimizing path are prescribed. We also note that minimal surfaces in 3-D were examined by Alava and Duxbury in the context of Ising models of magnets.⁽²²⁾

In the work of Jeulin⁽¹²⁾ the choice of the optimal path between two prescribed points (source and destination) was also solely determined by the minimum energy consumption criterion. This was motivated by considering the situation where the scale of variation of the stored energy field $G(x, y)$ is much larger than the scale of variation of the field $\gamma(x, y)$. This implies that variations in $G(x, y)$ can be disregarded, i.e.,

$$G(x, y) = G_0 = \text{const} \quad (5)$$

where G_0 should be viewed as an average (homogenized) value for the field $G(x, y)$.

We remark here that condition (5) is not necessarily sufficient for using the minimum energy consumption criterion only. Indeed, if relation (3) is not satisfied:

$$G_- < 2\gamma_{\max} \quad (6)$$

then the path $\bar{\Pi}(L)$ which minimizes the total fracture energy Γ may violate Eq. (1) for some edge e' . We treat this situation by introducing, in addition to the energy minimization criterion, a so-called *cost test* procedure for a constant field G_0 such that inequality (6) holds. This cost criterion accounts for unbreakable bonds: a physically realistic situation. Having chosen the path $\Pi_0(L)$ which minimizes the total fracture energy we check if

$$2\gamma(e) < G_0, \quad e \in \Pi_0(L) \quad (7)$$

If Eq. (7) is satisfied, then we are finished and $\Pi_0(L)$ is the OFP that we seek. Otherwise we pick the next path $\Pi_1(L)$ which minimizes total energy consumption among all other paths (joining the given point and plane) but $\Pi_0(L)$. Then we make the cost test (7) for the path $\Pi_1(L)$ and so on. We stop when (7) is satisfied. Unfortunately, this procedure is very expensive computationally. In order to study this effect within the framework of the minimum path algorithm, we choose to set some upper limit on the bond strength, after which the bond becomes “unbreakable,” and the path is forced to avoid those bonds. For distributions which have a wide range of bond strengths, this will approximate Griffith’s criteria reasonably well. At first glance, it appears that the cost test would allow one to incorporate

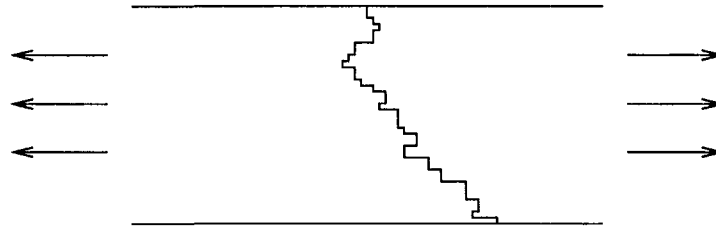


Fig. 2. Sample crack path. Note that the endpoint on the bottom is not fixed, but it is determined from the minimum energy path.

variations of the stored energy $G(x, y)$. However, $G(x, y)$ is usually a function of the current level of damage and therefore it is time dependent. Incorporation of the time dependence in an numerical algorithm would be a possible extension of our work.

We use mathematical ideas and results from first-passage percolation in the study of the fracture of brittle solids for two-dimensional materials. This includes the use of the wandering exponent ζ [defined by (16)], which characterizes the transversal deviation (roughness) of the fracture path (see Fig. 2) and the exponent χ [defined by (17)], which characterizes the fluctuations of the energy consumed by the path which fractures the specimen into two pieces. For our fracture model, we consider the exponents ζ and χ in the *semi-directed* sense (north, east or west orientation) since this reflects the fact that the fracture path does not like to reverse itself as observed by Jeulin.⁽¹²⁾ We have already noted that such exponents have arisen in variety of physical model^(16–18) and have been shown to be universal for different types of lattice orientations.⁽²³⁾ We note here that the exponents ζ and χ should not be viewed as critical in the sense that they were obtained under conditions specified in Eq. (10) below [compare to Eq. (11)].

In addition to the usual Bernoulli percolation lattice models, one can treat percolation on a square lattice with orientation in either a directed sense (north-east orientation) or a semi-directed sense (north, east or west orientation). The bonds (or sites) in the lattice are chosen to be occupied with some random probability p as in standard percolation, but clusters can only be formed by moving from bond to bond in one of the possible oriented directions. Because of this constraint, it becomes more difficult for an infinite cluster to form. As a consequence the percolation threshold for oriented Bernoulli percolation shifts upward from the usual value p_c , depending on the type of orientation, according to the inequalities

$$p_c < p_c^{\text{sdir}} < p_c^{\text{dir}} \quad (8)$$

where p_c^{sdir} and p_c^{dir} denote the thresholds for the semi-directed and directed cases, respectively. Similarly, the correlation length exponent ν , which characterizes the length scale of finite clusters in the system when it approaches the threshold from below [behaving as $(p_c - p)^{-\nu}$], satisfies the following inequalities for the aforementioned three types of orientations:

$$\nu < \nu^{\text{sdir}} < \nu^{\text{dir}} \quad (9)$$

We note here that ν for directed and semi-directed percolation is not isotropic but is a function of the direction in which it is measured. In this paper, we will always refer to ν for directed and semi-directed percolation *in the direction of "propagation"* (north for the former and north-east for the latter) and thus Eq. (9) applies only to such cases. One of the most striking features of critical phenomenon is the universality of the exponents. In particular, this means that ν , *for a particular orientation*, is independent of the lattice symmetry (e.g., its numerical value is the same for square, triangular, honeycomb and other lattices) and changes only with dimensionality of the system.

Although values of the percolation threshold and correlation length exponent are well established for usual percolation (see ref. 10 and references therein) and have been obtained more recently for directed percolation,^(10, 24) very little is known about the critical parameters for semi-directed percolation. In the next section, we will determine these critical properties in the semi-directed case. Subsequently, we will ascertain whether the exponents ζ and χ remain universal in the vicinity of the semi-directed Bernoulli percolation threshold p_c^{sdir} .

We will also study numerically several issues which raise theoretical questions to be addressed in future mathematical studies of first-passage percolation and related topics. One such question is that of the fractal dimension of the OFP at criticality. An important mathematical condition under which most statements in the first-passage percolation are proven is non-percolation of zeros. This means that if $\gamma(e)$ are identically distributed random variables (i.i.d's) taking values say in the interval (0, 1), then

$$P(\gamma(e) = 0) < p_{cr} \quad (10)$$

where P stands for the probability and p_{cr} refers to the percolation threshold of zeros. For a simple binary model with values 0 (pores) or 1 (solid), this, roughly speaking, means that the specimen is not broken. It was shown in ref. 9 that under this condition (and some other technical condition on the second moments), the length of the first-passage path

between the two points a distance L apart scales as L for large L . By means of numerical simulations, we show in this work that at criticality, i.e., when

$$P(\gamma(e) = 0) = p_{cr} \quad (11)$$

the path scales as L^α , with $1 < \alpha < 2$, i.e., the OFP becomes fractal for point-to-plane first-passage percolation. In fact the situation corresponding to Eq. (11) makes sense physically. Indeed, since according to well-known results in two dimensions the zero energy path does not exist with positive probability (see ref. 25 and references therein) which is equal to 1/2 for the square lattice (also, there is no infinite cluster at criticality) and therefore the specimen is not quite broken with significant probability. We remark here that fractal dimension of various paths at criticality was reported in many studies. In this sense our result is not at all surprising but rather consistent with previous work. However, it is a challenging problem to find analytically nontrivial upper and lower bounds for α or even prove rigorously that $0 < \alpha < 1$ (see note added in proof).

When a major crack fractures a specimen into two pieces, one can observe two limiting scenarios. First, during the process of formation of this major crack, there may be instances in which many other processes off the crack path are also formed. In this case, the fracture energy differs significantly from the energy consumed by the major crack. Another limiting case is when the major crack dominates and off-path processes consume a negligible amount of energy. The realization of these limiting scenarios depend on material properties and the distribution of the inhomogeneities. For the class of materials in which the second scenario applies, we will answer a basic question: how does the fracture energy (simply related to the fracture toughness⁽²¹⁾) depend on the degree of inhomogeneity of the specimen?

III. DETERMINATION OF CRITICAL PARAMETERS FOR SEMI-DIRECTED BERNOULLI PERCOLATION

We consider a model of semi-directed Bernoulli percolation in which the bond strengths are zero or unity and determine the critical parameters p_c and ν , which strictly speaking are defined for infinite systems. In order to determine them via simulations of finite systems, we must first understand how these quantities behave as a function of system size. Perhaps the most straightforward way to measure ν for a finite size system is to measure the width $A(L)$ of the percolation transition for a system of linear size L . This percolation transition is defined by plotting the percolation probability $P(p, L)$ as a function of the bond occupation probability p for a

given L . This resulting curve is roughly sigmoidal in shape, but the rise in the curve from 0 to 1 is not discontinuous. Instead, it is a smooth transition which occurs over some width $\Delta(L)$. For a reasonable definition of the transition width (see, for example ref. 10), $\Delta(L)$ should scale as

$$\Delta(L) \propto L^{-1/\nu} \quad (12)$$

We will define more precisely how we choose to define our transition width below in Eq. (15).

For a finite sized system of size L , one can define an effective percolation threshold $p_c^{\text{eff}}(L)$ as the occupation probability at which some fraction (typically 1/2) of the systems contain clusters which span the entire length of the system. As $L \rightarrow \infty$, $p_c^{\text{eff}}(L) \rightarrow p_c$. One can extract $p_c^{\text{eff}}(L)$ for a given L from the plot of the percolation probability $P(p, L)$ by fitting some smooth curve through the points at determining at what point 1/2 (or some other fraction) of the samples percolate, i.e., $p_c^{\text{eff}}(L)$ is the value of p such that

$$P(p_c^{\text{eff}}(L), L) = 1/2 \quad (13)$$

Once these values have been calculated we can take advantage of another scaling relation⁽¹⁰⁾ which states

$$p_c^{\text{eff}}(L) - p_c \propto L^{-1/\nu} \quad (14)$$

using the value of ν calculated previously. A plot of the probability $p_c^{\text{eff}}(L)$ vs. $L^{-1/\nu}$ will result in a graph which intersects the vertical ($p_c^{\text{eff}}(L)$) axis (where $L = \infty$) at p_c .

Our estimations of p_c and ν for our binary semi-directed Bernoulli percolation model were done via finite size scaling using lattices of size L , where $200 \leq L \leq 2000$. We found there were significant finite-size effects for $L < 200$ (i.e. in these cases the values of L were small enough that the asymptotic scaling laws did not describe the behavior completely). Our values of $\Delta(L)$ and $p_c^{\text{eff}}(L)$ were extracted by fitting each curve to a function of the form

$$P(p, L) = \frac{1 + \text{erf}[(p - p_c^{\text{eff}}(L))/\Delta(L)]}{2} \quad (15)$$

An example of such a fit for $L = 1500$ is shown in Fig. 3. This curve could also have been fit to similar functions, such as the hyperbolic tangent. We chose the error function because the resulting plot more closely fit the error function, but using the hyperbolic tangent to obtain $\Delta(L)$ and $p_c^{\text{eff}}(L)$ did not change the results significantly, especially in the case of $p_c^{\text{eff}}(L)$.

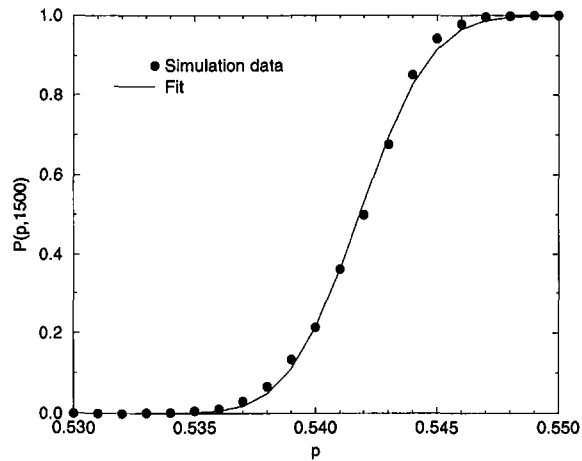


Fig. 3. Example of the determination of $p_c^{\text{eff}}(L)$ and $\Delta(L)$ for $L = 1500$ for the semi-directed binary model. The fitting function is defined in Eq. (15).

The resulting plot of $\Delta(L)^{-1}$ vs. L is shown in Fig. 4. (Lattices with larger values of L were not used because their width was more difficult to ascertain due to the sharpness of the transition.) The slope of the line is 0.665 ± 0.002 , which corresponds to a value of $\nu^{\text{sdir}} = 1.50 \pm 0.01$. Our numerics suggests that ν^{sdir} is exactly the simple fraction $3/2$, which lies

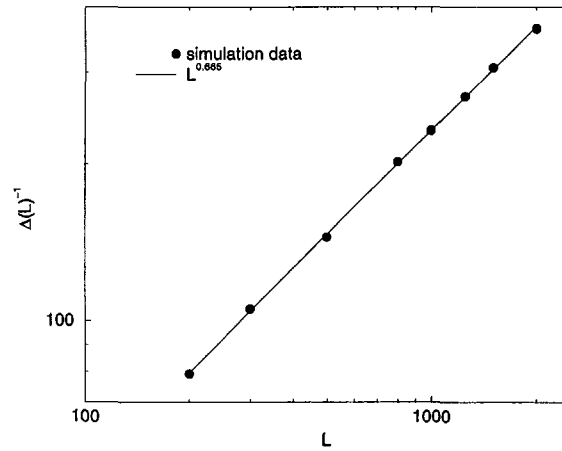


Fig. 4. A plot of the scaling of the inverse transition width $\Delta(L)^{-1}$ as a function of L for the semi-directed binary model. The circles are the simulation data while the line represents a best fit power-law. The power law has an exponent of 0.665 ± 0.002 , which is very close to $2/3$.

between the corresponding known values (described below) for usual and directed Bernoulli percolation.

Why should the value of ν^{sdir} lie in between the values of ν and ν^{dir} in two dimensions? Indeed, this is consistent with other known percolation results. For example, for usual Bernoulli percolation,⁽¹⁰⁾ we have that $\nu = 4/3$ for two-dimensional systems and $\nu \approx 0.88$ for three-dimensional systems. Thus, we conclude that adding the degrees of freedom may lead to a decrease in the numerical value of the correlation length exponent (at least below the upper critical dimension). Recall that the correlation length behaves as $(p - p_c)^\nu$ as p approaches p_c . Since p is the fraction of occupied bonds, adding degrees of freedom (e.g., relaxing the orientational constraints or moving to a higher dimension) means that the contribution from each bond becomes less significant. Therefore, it is natural to expect that the value of ν decreases when the degrees of freedom increase.

Using our evaluation of ν for the semi-directed case, we can now plot $p_c^{\text{eff}}(L)$ vs. $L^{-1/\nu}$. Fig. 5 shows that if we fit this to a straight line and extrapolate to $L = \infty$, we get a value of 0.5475 ± 0.0025 for p_c^{sdir} . As we can see from the figure, the difference between the value of p_c^{sdir} and the values of $p_c^{\text{eff}}(L)$ for finite L is significant, and the extrapolation is required to get an accurate answer. It is useful to compare our new results for semi-directed percolation to those of standard percolation,⁽¹⁰⁾ where $p_c = 0.5$ and $\nu = 4/3$, and for directed percolation,^(10, 24) where $p_c^{\text{dir}} = 0.6447$,⁽²⁴⁾ $\nu^{\text{dir}} = 26/15$. The determination that $\nu^{\text{dir}} = 26/15$ is based on numerics.

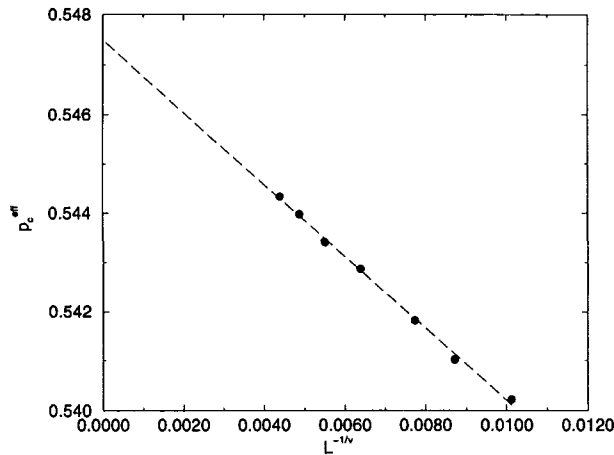


Fig. 5. A plot of p_c^{eff} vs. $L^{-1/\nu}$ for the semi-directed binary model. The circles are the simulation data, while the dashed line is a best fit line to the data. It intersects the y -axis at 0.5475 ± 0.0025 , which represents the value of p_c for the infinite system.

IV. OPTIMAL FRACTURE PATH (OFP) STATISTICS FOR POINT-TO-PLANE CRACKS

The wandering exponent ζ is defined as the exponent which controls how the “width” $w(L)$ of the crack (as defined below) scales as a function of system size L , i.e.,

$$w(L) \propto L^\zeta \quad (16)$$

In this paper, the width was defined in three different ways, as discussed below. The energy fluctuation exponent χ is simply defined as

$$\Delta E(L) \propto L^\chi \quad (17)$$

where ΔE is the standard deviation of the distribution of crack energies for a given L . To test our numerical code, we first evaluate the known exponents ζ and χ in the semi-directed model away from criticality (for different lattices). We then determine them in the vicinity of the percolation threshold.

We measured values of ζ and χ by scaling the width and energy fluctuations, respectively, as a function of system size L . This was done by assigning random breaking energies to the nearest-neighbor bonds of an $4L$ (x -direction) by L (y -direction) square lattice based on three given distribution described below. Then, the path between the point $(2L, L)$ and the edge $y=0$ which contained the smallest total sum of bond strengths was determined using Dijkstra’s algorithm.⁽²⁶⁾ This algorithm is an iterative one in which one starts at a specific site, and then at every step the next “closest” site to the original one (in terms of the given metric) is determined. The procedure is repeated until a site on the opposite edge is found. The lattice was chosen to be four times larger in the x direction in order to prevent the path from going outside the box in the horizontal direction. For a few of the smaller L cases, the lattice was chosen to be eight times larger in the x direction.

For each value of L , these minimum energy paths were determined for a large number of samples, ranging from 10^5 for $L=10$ to 1000 for $L=224$. For each sample, we found the average total energy and length of each path. We also found the average “width,” with the width defined in three ways. The first way was the “start-stop” width which represented the x displacement between the beginning and end point. The second was the maximum width, which is defined as the displacement between the maximum and minimum point on the path in the x direction. The final definition was simply the radius of gyration of the path in the x direction. As this average weights all of the points on the path in a more equal manner than

the first two, we found it to have the best scaling properties. Unless otherwise specified, this is the definition of path width that is presented in the results.

We have studied systems with three different bond distributions. The first system contained bonds with a uniform distribution of strengths, ranging from 0 to 100. The second system contained bond strengths which were Gaussian distributed with a mean of 50 and a width of σ (the bonds whose values were originally less than 0 were set equal to 0). The third distribution was started with a system of uniformly distributed bonds like the first, but then a critical fraction (equal to $1 - 0.5475$ for our case of semi-directed percolation) were set equal to zero. The fraction of occupied bonds was therefore 0.5475, as determined previously.

One initial test of our systems was to check the universality of the exponents ζ and χ for the OFP in our different systems. These studies were done using only an energy minimization, and not taking into account Griffith's criterion. The results of these studies are plotted in Fig. 6 (mean-square width) and Fig. 7 (energy fluctuations). The system with the uniform distribution of bond strengths yielded results which are numerically identical to the known values $\zeta = 2/3$ and $\chi = 1/3$. In the case of the bonds with a Gaussian distribution of strengths, the transverse width measurements do not show a clear power law behavior for the sample sizes used, but do seem to be asymptotically approaching a slope of $2/3$ in the log-log plot of width vs. L . The energy fluctuations for this sample still showed a power law behavior corresponding to an exponent of $\chi = 1/3$. We

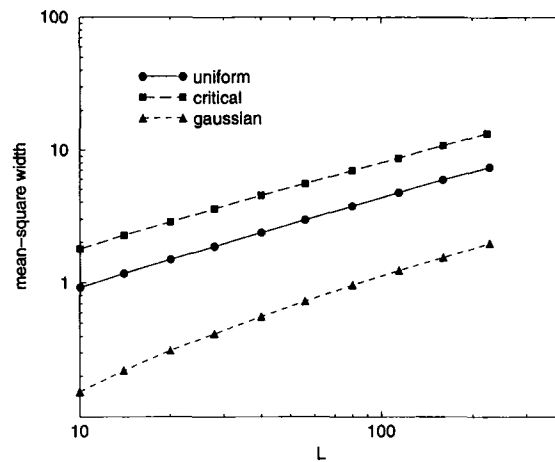


Fig. 6. Plot of the crack mean-square width as a function of L for three cases. Although the magnitudes are different, all show approximately the same exponent for large L .

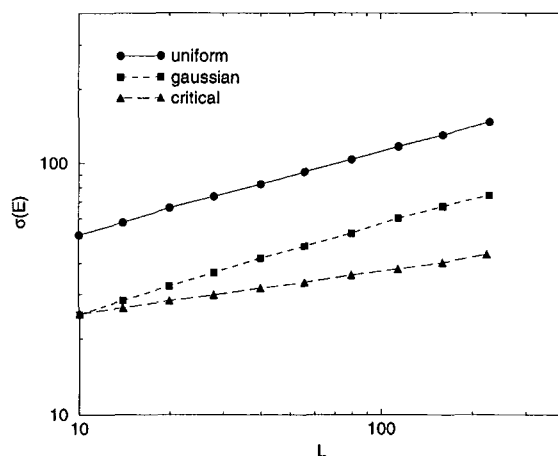


Fig. 7. Plot of the standard deviation in the distribution of fracture energies as a function of L for three cases. The two non-critical cases give similar exponents of approximately $1/3$, while the critical case gives a significantly smaller value.

note that the values of ζ and χ are the same not only for different lattices but also stay the same for random mosaics. Thus, our simulations produced exponent values which are consistent with previous studies on directed polymers,⁽¹⁶⁾ solid-on-solid model,⁽¹⁸⁾ and the fuse and elastic-perfect-plastic models,⁽¹⁹⁾ and hence validated our numerical technique.

The case of the nearly critical sample is an interesting one. Because of all of the zero strength bonds, this sample could be thought of physically as being practically broken, and held together by only a few bonds (“very spongy” specimen). In this case, ζ is still close to $2/3$ (although for small values of L there is some deviation from power-law behavior), but χ becomes approximately 0.17 , which is about half of what it was for the non-critical case. Thus we see that the well known scaling relation $\chi = 2\zeta - 1$ (see e.g., ref. 27 and references therein), which holds under condition Eq. (10), is no longer true. In fact, it is easy to see that a simple heuristic argument for the latter scaling relation based on the Pythagorean theorem⁽²⁸⁾ applied to a right triangle with the hypotenuse $L + L^\zeta$ and legs L and L^ζ does not work in the vicinity of the percolation threshold, which supports our numerical results. Indeed, this heuristic picture assumes that the boundary of the area wetted at time t by the fluid, which is supplied at the origin, roughly grows as a smooth surface perturbed by small oscillations. However, in the vicinity of the threshold, large clusters of zeros can be added at once and therefore the latter assumption is no longer applicable.

With the values for the sample without the *cost-test* algorithm determined, we can now calculate similar quantities using the *cost-test* procedure

described earlier. In this case, we will use the uniform distribution of bond strengths, where the strengths vary between 0 and 100, but the path will not be allowed to break any bond with a strength greater than 80. So, in general, the path will contain lower energy bonds, but it will be longer since it will have to avoid 20% of the bonds. In the simulation, if the starting point was such that the crack was “trapped” by a system of unbreakable bonds, that sample was rejected. The results for the width change simulation are shown in Fig. 8. The slope for this graph is approximately 0.66, but the values are slightly larger, due to the bonds which must be avoided. The associated energy fluctuations also follow the same trend, with the exponent being approximately $1/3$, but the values themselves are about 2% higher. Although this difference is small it occurs for all values of L . Thus, we conclude that the cost test does not change the qualitative picture but only changes the actual numbers.

In order to determine the fractal dimension of the path α , we plotted the total path length vs. L for the same samples that were used in the study of ζ and χ . A log-log plot of these results are shown in Fig. 9. The line fitted to the data shows a best fit power law that gives an exponent $\alpha = 1.03 \pm 0.01$, where α represents the fractal dimension of the path. This is very close to 1, but different enough to suggest that the path may be fractal.

A final measurement is that of the dependence of the normalized fracture energy $E(L)/L$ of the OFP on the width of the *distribution of the specific energy of bond strengths*. In other words, how does the degree of

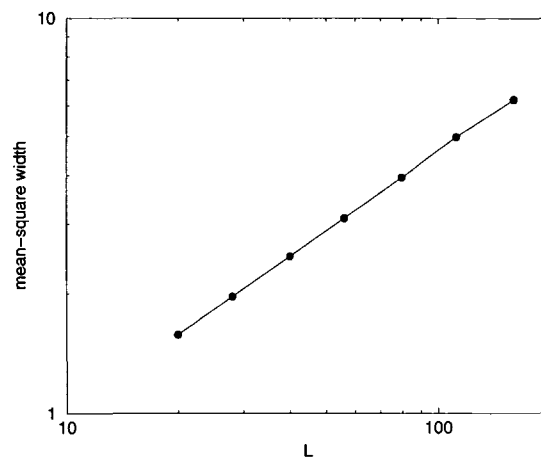


Fig. 8. Plot of the crack mean-square width as function of sample size when the cost testing is included. The slope is still approximately $2/3$, but the values are higher due to the “unbreakable” bonds.

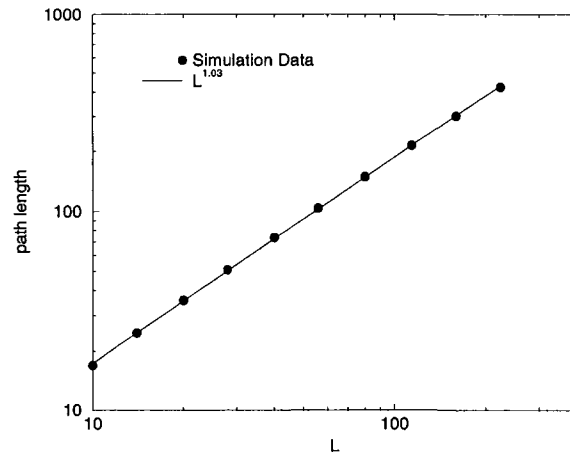


Fig. 9. Plot of the total path length as a function of L for the critically dilute case. The slope of this line of 1.03 ± 0.01 and represents the fractal dimension a of the path in this case.

inhomogeneity among the different bonds in the system affect the path energy, if the type of distribution is the same. To test this, we used a Gaussian distribution of bond strengths, centered at 50. As in the previous case, if a negative bond strength was drawn from the distribution, it was set equal to 0. For the distribution widths of interest, this happened very infrequently. Fig. 10 shows the results of this simulation, which was performed on lattices

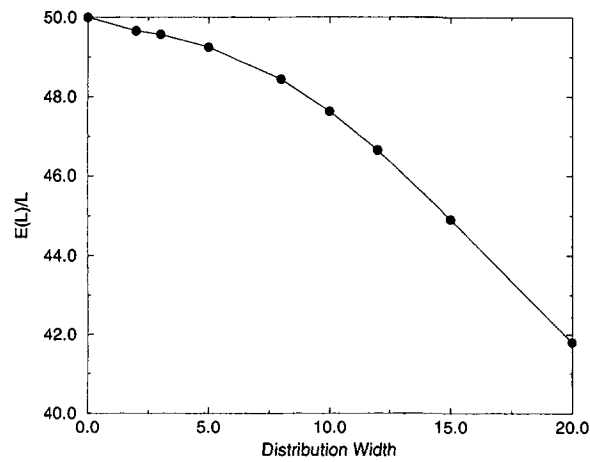


Fig. 10. Plot of the total fracture path energy vs. distribution width. The dependence is roughly quadratic for small values of distribution width.

with $L = 160$. For each width, the energy given is the average over 1000 different configurations. From the graph, we see a dependence that is approximately quadratic in nature for small values of the width. It would be interesting to determine the precise theoretical dependence of the energy decrease as a function of distribution width. The small width case is at least conceivably within the reach of being proved rigorously using perturbation theory considerations. For some restricted class of materials in which the major crack dominates, these results can be used to determine the fracture toughness which is related to the fracture energy in a simple way.⁽²¹⁾

We also carried out similar measurements of the normalized energy of the OFP versus the width of the distribution of bond strengths for uniform distributions. Although the data for these simulations were more limited in number, we again observed a quadratic dependence for small values of width. In this case, the width was just simply the difference between the two endpoints of the uniform distribution. This implies that the quadratic behavior for small widths could be a universal phenomenon for a large class of bond distributions.

V. CONCLUSIONS

We have interpreted the well-developed model of semi-directed first-passage percolation and associated universal exponents ζ and χ in the context of the fracture two-dimensional brittle materials under quasi-static loading. In particular, we studied the interplay between semi-directed first-passage percolation model (also known in the statistical physics literature as directed polymers) and semi-directed Bernoulli percolation by determining the exponents in the vicinity of the percolation threshold for the semi-directed model. This study led to a number of new results. First, we determined the critical parameters p_c^{dir} and ν^{dir} for semi-directed Bernoulli percolation. We found that the critical fraction of occupied bonds is $p_c^{\text{dir}} = 0.5475$ (for a simple binary model) and our numerics suggest that correlation length exponent ν^{dir} is exactly $3/2$. We observed that this value lies between the corresponding values for usual and directed Bernoulli percolation. We also observed that the well-known scaling relation $\chi = 2\zeta - 1$ between the wandering exponent ζ and energy fluctuation exponent χ breaks down in the vicinity of the percolation threshold and provide a heuristic explanation for this behavior. This analysis of the crack statistics was carried out for a wide variety of bond strength distributions, including that of an almost critical distribution of zero-strength bonds.

For a restricted class of materials, we studied the dependence of the fracture toughness on the width of the distribution (i.e., degree of inhomogeneity) of the specific fracture energy. This dependence was found to be

quadratic for small widths and two different distributions (uniform and Gaussian), suggesting that this dependence may be universal. We have also measured the fractal dimension of the cracks for the almost critically broken samples and have numerical evidence that they are fractal, which is consistent with other fractal paths reported in many numerical studies. Finally, we observe that taking into account Griffith's criteria does not change the scaling exponent but changes the constants.

ACKNOWLEDGMENTS

We thank C. Newman for many useful discussions of first-passage percolation. We are indebted to the referees whose comments and constructive criticisms of the paper led to significant improvements and clarification of several issues. S. T. and M. D. R. gratefully acknowledges the support of the Air Force Office of Scientific Research under Grant F49620-92-J-0501. Much of this work was done while L. B. was visiting Princeton University and he is grateful to S. T. for his hospitality and the financial support (AFOSR grant) that he received there. He also acknowledges partial support by NSF grant DMS-9622927.

NOTE ADDED IN PROOF

After this paper was accepted for publication, we were made aware of a preprint by Aizenman and Burchard. In this work, several interesting results on critical behavior (including the fractal dimension of the shortest path) have been rigorously proven.

REFERENCES

1. A. A. Griffith, *Phil. Trans. R. Soc.* **221A**:163 (1920).
2. C. Inglis, *Transactions of the Institute of Naval Architects* **55**:219 (1913).
3. G. Irwin, *Fracturing of Metals* (American Society for Metals, Cleveland, 1948), pp. 147–166.
4. *Continuum Damage Mechanics Theory and Applications*, D. Krajcinovich and J. Lamaitre, eds. (Springer, New York, 1987).
5. B. Lawn, *Fracture of Brittle Solids* (Cambridge Press, New York, 1993).
6. H. Hermann and S. Roux, *Statistical models for the fracture of disordered materials* (North-Holland, Amsterdam, 1990).
7. P. Duxbury and P. Leath, *Phys. Rev. B* **49**:12676 (1994).
8. G. Grimmett, *Percolation*. (Springer-Verlag, New York Berlin, 1989).
9. H. Kesten, *Aspects of first passage percolation*, Lecture Notes in Mathematics (Springer-Verlag, Berlin, 1986).
10. D. Stauffer and A. Aharony, *Percolation Theory* (Taylor & Francis, London, 1994).

11. A. Delaplace, G. Pijaudier-Cabot, and S. Roux, *J. Mech. Phys. of Solids* **44**:99 (1996).
12. D. Jeulin, *Engineering computations* **10**:81 (1993).
13. C. Lisea, C. Newman, and M. Piza, *Probability Theory and Related Fields* **106**:559 (1996).
14. E. Bouchard, *J. Phys. Condens. Mat.* **9**:4319 (1997).
15. C. Newman, in *Proceedings of the International Congress of Mathematics*, S. D. Chatterji, ed. (Birkhauser, Basel, 1995), Vol. 2, pp. 1017–1023.
16. M. Kardar and Y. Zhang, *Phys. Rev. Lett.* **58**:2087 (1987).
17. D. Huse, C. Henley, and D. Fisher, *Phys. Rev. Lett.* **55**:2923 (1985).
18. J. M. Kim and J. M. Kosterlitz, *Phys. Rev. Lett.* **62**:2289 (1989).
19. A. Hansen, E. Hinrichsen, and S. Roux, *PRL* **66**:2476 (1991).
20. D. Jeulin, *Appl. Mech. Rev.* **47**:141 (1994).
21. R. J. Young and P. A. Lovell, *Introduction to Polymers* (Chapman & Hall, New York, 1991).
22. M. J. Alava and P. M. Duxbury, *Phys. Rev. B* **54**:14990 (1996).
23. C. Newman and M. Piza, *Ann. Prob.* **23**:977 (1995).
24. R. Baxter and A. Guttmann, *J. Phys. A* **21**:3193 (1988).
25. R. Langlands, P. Pouliot, and Y. Saint-Aubin, *Bull. Am. Math. Soc.* **30**:1 (1994).
26. V. Chvátal, *Linear Programming* (W. H. Freeman, New York, 1983).
27. J. Krug and H. Spohn, in *Solids far from equilibrium: growth, morphology and defects*, C. Godrèche, ed. (Cambridge University Press, New York, 1991), pp. 479–582.
28. C. Newman, private communication.